Korean J. Chem. Eng., 37(3), 536-545 (2020)
DOI: 10.1007/s11814-019-0448-y

pISSN: 0256-1115
eISSN: 1975-7220

Efficient photocatalytic degradation of 2-chloro-4,6-dinitroresorcinol in salty industrial wastewater using glass-supported TiO_2

Yuan Zhang*,, Wenwei Jiang***, Yongsheng Ren****, Baoming Wang*,**,†, Yong Liu*,**, Quanxian Hua*,**, and Jianwei Tang*,****

*School of Chemical Engineering, Zhengzhou University, Zhengzhou 450001, China
**National Research & Popularization Center for Calcium, Magnesium, Phosphate & Compound Fertilizer Technology, Zhengzhou 450001, China
***School of Chemical Engineering, Sichuan University, Chengdu 610065, China
****State Key Laboratory of High-efficiency Utilization of Coal and Green Chemical Engineering, Ningxia University, Yinchuan750021, China
(*Received 31 August 2019 • accepted 1 December 2019*)

Abstract−2-chloro-4,6-dinitroresorcinol (CDNR) is detrimental to the environment and human health owing to its high toxicity and poor biodegradability. To demonstrate the feasibility of photocatalytic degradation of CDNR from industrial salty wastewater by borosilicate glass supported TiO_2 under UV light irradiation, borosilicate glass supported TiO_2 was prepared successfully by a novel sol-gel route via dip-coating method and characterized by XRD, SEM, FTIR and XPS analysis. The results showed that TiO_2 catalyst has the anatase phase structure with crystallite size of 11.5 nm and coats uniformly on the borosilicate glass. Also, the effects of reaction time, pH value, TiO_2 dosage, CDNR concentration, and Cl^- on the degradation efficiency of CDNR were investigated. The results indicated that at pH 2, reaction time 3.5 h, CDNR concentration 10 mg/L, NaCl concentration 5.85% (w/w) and TiO_2 dosage 1.0 g/L, 97.7% of CDNR was degraded in the presence of Cl^-, this corresponded to a rate constant of 1.05 h^{-1}, illustrating the feasibility of photocatalytic degradation process. This contribution provides a basic investigation regarding the potential application of borosilicate glass supported TiO_2.

Keywords: Photocatalytic Degradation, 2-Chloro-4,6-dinitroresorcinol, Wastewater, Anatase, Titanium Dioxide

INTRODUCTION

2-Chloro-4,6-dinitroresorcinol (CDNR) is an important intermediate for synthesizing the monomer for producing Poly-phenylene benzobisoxazole (PBO) [1-3]. PBO fiber due to high tensile strength and outstanding thermal stability, known as a novel super high performance fiber in the 21st century, has been widely adopted in the aeronautics, aerospace and military fields [4,5]. However, CDNR belonging to dinitrophenolic compounds is detrimental to the environment and human health due to high toxicity, carcinogenicity and poor biodegradability [6], and is included in the National Hazardous Waste List by the Chinese Ministry of Environmental Protection; the limit for CDNR is 1 mg/L. According to the conventional manufacturing process, the synthesis process of CDNR is typically based on aqueous alkaline hydrolysis of 4,6-dinitro-1,2,3-trichlorobenzene, thus generating considerable amounts of the wastewater containing CDNR and NaCl [1,2,7]. The wastewater containing CNDR and NaCl could give rise to numerous adverse effects on the aquatic ecosystem and human health when it is discharged into the aquatic environment. In view of this, CDNR must be removed prior to discharging into water bodies. To date, few studies concerning CDNR degradation have been reported [8]. Our research efforts have been undertaken to reduce CDNR in wastewater by adsorption method. Unfortunately, we did not resolve the problem in a satisfactory way by the above method. Considering the safety of the aquatic environment, the degradation process for CDNR must be highly efficient. As a response, the development of an efficient and eco-friendly method to degrade CDNR has become imperative.

Advanced oxidation processes (AOPs) are considered a potential method to degrade a wide range of persistent organic pollutants by accelerating the non-selective oxidation [9]. So far, the mineralization of recalcitrant organic environmental pollutants into harmless products through heterogeneous photocatalysis with TiO_2 as photocatalyst is the most studied oxidation process and has a widely demonstrated efficiency. UV-light irradiation generates photons whose energy is equal to or greater than the band gap energy (EG= 3.2 eV) for TiO_2. When TiO_2 is irradiated with the photons, electron-hole pairs are created. In an aqueous system, holes react with H_2O or OH^- adsorbed on the surface of TiO_2 to produce HO· which are the most oxidizing species in this process. The photocatalysis principle of TiO_2 is mainly based on the hydroxyl radical generation through the e^-/h^+ pairs generated under UV light irradiation at mild temperature and pressure [10-15]. Besides, TiO_2 possesses good photocatalytic efficiency, high chemical stability, low cost and nontoxicity [16,17]. However, in many cases, the treatment process

†To whom correspondence should be addressed.
E-mail: ziqiangdere@126.com

by TiO_2 photocatalysis is unfeasible because it is difficult to separate and recycle the TiO_2 nanoparticles from treated water after reaction. Immobilizing nanoparticles on glass has been reported to overcome the difficulties in the separation [18,19]. Therefore, the preparation of highly photoactive TiO_2 on glass is necessary for realistic applications of TiO_2 photocatalysis in wastewater treatments.

The photocatalysis by TiO_2 has been studied in previous studies for the degradation of some phenolic compounds, such as phenol [20,21], 4-chlorophenol [22], 2,4-dichlorophenol, 2,5-dichlorophenol, 2,4,5-trichlorophenol, 4-nitrophenol, 2-nitrophenol, 2,4-dinnitrophenol [23], 2-sec-butyl-4,6-dinitrophenol [6,24,25]. However, to the best of our knowledge, the potential application of TiO_2 in the degradation of CDNR has not been investigated in the literature yet. In the present paper, TiO_2 sol was readily prepared with cheap titanium oxysulfate as raw material at low temperature by an improved sol-gel method [8,26]. To overcome the difficulty in separation and recycle, borosilicate glass supported TiO_2 was obtained by dip-coating. The feasibility of degrading CDNR from wastewater using borosilicate glass supported TiO_2 was studied. The effects of reaction time, pH value, TiO_2 dosage, CDNR concentration, and Cl^- were studied. The degradation kinetics of CDNR was also preliminarily investigated in this work.

MATERIAL AND METHODS

1. Chemicals

Borosilicate glass blades with size 3.8 cm×2.5 cm used as a support for TiO_2 were purchased from Chengdu Lingyun Glass Factory. 2-chloro-4,6-dinitroresorcinol (CDNR) was used as a dinitroresorcinol pollutant and prepared in our laboratory. All other chemicals used, including dehydrate titanyl sulfate ($TiOSO_4 \cdot 2H_2O$), ammonium hydroxide ($NH_3 \cdot H_2O$), hydrogen peroxide (H_2O_2), sodium chloride (NaCl), acetone, sodium hydroxide (NaOH), hydrogen chloride (HCl) and barium chloride ($BaCl_2$), were of analytical grade and purchased from Chengdu Kelong Chemical Co., Ltd., China. All the chemicals were used as received. Deionized water was used throughout the experimental work. Aqueous solutions with different CDNR and NaCl concentrations were prepared by dissolving CDNR and NaCl in deionized water.

2. Preparation of Borosilicate Glass Supported TiO_2

Borosilicate glass supported TiO_2 was prepared by the sol-gel route via dip-coating method [8,26]. The borosilicate glass substrate was carefully sonicated in acetone and deionized water, respectively, and then immersed in 10% (w/w) NaOH solution and 10% (w/w) HCl for 5 min under ultrasonic conditions, respectively. The borosilicate glass substrate was cleaned to neutral with deionized water after each sonication [27]. The peroxo titanic acid (PTA) sol was prepared with 0.2 mol/L titanyl sulfate, 25-28% ammonium hydroxide and 30% H_2O_2. 25-28% ammonium hydroxide was added to 0.2 mol/L titanyl sulfate solution to adjust the pH of the system to 8-9, the formed precipitate was washed with deionized water until no SO_4^{2-} could be detected. SO_4^{2-} was detected by precipitation method through adding $BaCl_2$. Then the precipitate was added into five-times of water, and 30% H_2O_2 was added dropwise to dissolve the precipitate until $n(H_2O_2) : n(Ti)=4 : 1$, then the system was aged for 24 h under magnetic stirring [28]. Then PTA sol was heated at 100 °C for 6 h under refluxing conditions and subsequently the resultant was designated as TiO_2 sol. Afterwards, the borosilicate glass substrate cleaned was dipped in TiO_2 sol and lifted at a velocity of 2 mm/s, dried at 100 °C for 2 h in an oven, and cooled to room temperature. The above procedure of dipping and drying was repeated until the amount of TiO_2 on the borosilicate glass substrate was increased to the related TiO_2 dosage. Hereafter the TiO_2 immobilized on borosilicate glass substrate is referred to as borosilicate glass supported TiO_2.

3. Characterization of Photocatalysts

The obtained TiO_2 sol was dried at 100 °C for 2 h and ground into powder. To identify the crystalline phase of the prepared TiO_2 powders, X-ray powder diffraction (XRD) analysis was performed by DX-2700 X-ray diffractometer (Dandong Haoyuan Instrument Co., Ltd., China) with a Cu Kα radiation source in the 2θ from 20° to 80°. The surface morphology and structure of borosilicate glass supported TiO_2 was checked by scanning electron microscope (SEM, JSM-7500F, Japan Electron Co., Ltd., Japan). Fourier transform infrared spectra (FT-IR) analysis were taken with a FTIR-8400S spectrometer (Shimadzu Corporation, Japan) to characterize elements' bonds with wavenumber varying from 4,000 to 400 cm^{-1}. X-ray photoelectron spectra (XPS) were recorded with an x-ray photoelectron spectrometer (Kratos Corporation, UK) to analyze the chemical bonding of TiO_2 powders.

4. Photocatalytic Degradation of CDNR

Photocatalytic degradation experiments were conducted in a 50 mL cylindrical Pyrex photoreactor for photocatalytic degradation of CNDR with the borosilicate glass supported TiO_2 and irradiation source promoted by UV lamp. According to the band gap energy (E_G=3.2 eV) for TiO_2, a UV lamp generates photons whose energy is equal to or greater than 3.2 eV. Besides, the photons absorbed by CDNR should be as little as possible. So, a UV lamp with wavelength of 253.7 nm was selected.

Photocatalytic reactions were performed at 25 °C and atmospheric pressure by the following procedure. First, the initial pH of wastewater was adjusted to the required value by adding a dilute aqueous of HCl or NaOH and measured with a pH meter. Then 20 mL wastewater with the corresponding CDNR and NaCl concentrations was poured into the photoreactor and then the required borosilicate glass supported TiO_2 was immersed in the wastewater. The wastewater was subjected to UV irradiation from UV lamp (λ=253.7 nm, 25 W) and treated as the starting point (t=0) of the photocatalytic degradation reaction, where the concentration of CDNR was designated as C_0. Degradation wastewater was withdrawn at a given time.

The concentration of remaining CDNR was analyzed by measuring the absorbance at a wavelength of 330 nm using a UV spectrophotometer. To evaluate the performance of the photocatalytic degradation, the percent degradation efficiency (η) of CDNR was defined as:

$$\eta(\%) = \frac{C_0 - C}{C_0} \times 100 \quad (1)$$

where C_0 and C are the concentration of CDNR at t=0 and t, respectively. A higher η value is associated with a higher degradation efficiency of CDNR.

To assess the degradation feasibility of CDNR in wastewater using borosilicate glass supported TiO_2, the factors affecting degradation efficiency of CDNR were investigated during the degradation process, such as reaction time (0-3.5 h), pH value (2-12), TiO_2 dosage (0.5-2.5 g/L), CDNR concentration (10-30 mg/L) and NaCl (0-5.85%).

5. Recycle of Borosilicate Glass Supported TiO_2

After the first photocatalytic degradation of CDNR by the borosilicate glass supported TiO_2, the borosilicate glass supported TiO_2 was taken out from degradation wastewater by tweezers and reused for degradation of another fresh wastewater under the same conditions. This procedure was repeated eight times to evaluate the stability and recycle of borosilicate glass supported TiO_2.

RESULTS AND DISCUSSION

1. Characterization of the Catalysts

1-1. XRD

To confirm the formation of TiO_2 crystals, the prepared photocatalysts were subjected to XRD. The wide-angle X-ray diffraction (XRD) pattern of the prepared TiO_2 photocatalysts is depicted in Fig. 1. The result revealed the crystal pattern of TiO_2. The XRD pattern of TiO_2 showed notable and well-resolved diffraction peaks when 2θ value was 25.3°, 37.9°, 48.1°, 54.1°, 62.8°, 70.1° and 75.3°, respectively. These diffraction peaks were in good accordance with the standard XRD pattern of anatase TiO_2 (JCPDS No.21-1272). No additional diffraction peaks attributed to impurity and rutile type confirmed the formation of the highly pure anatase TiO_2. Similarly, pure anatase TiO_2 was synthesized by sol-gel method in a previous study [29]. However, compared to the conventional sol-gel method, amorphous TiO_2 was changed into anatase structure at low reflux temperature in this study. The XRD peak at 2θ=25.3° is often taken as the characteristic peak of anatase (101) crystal phase [24]. The diffraction XRD pattern for the prepared TiO_2 particles presented high crystallinity through the characteristic broad peak. The average crystal size of the prepared TiO_2 photocatalyst was estimated from the peak width at half maximum for the highest peak in the XRD diffractograms according to the following Scherrer's equation [30,31]:

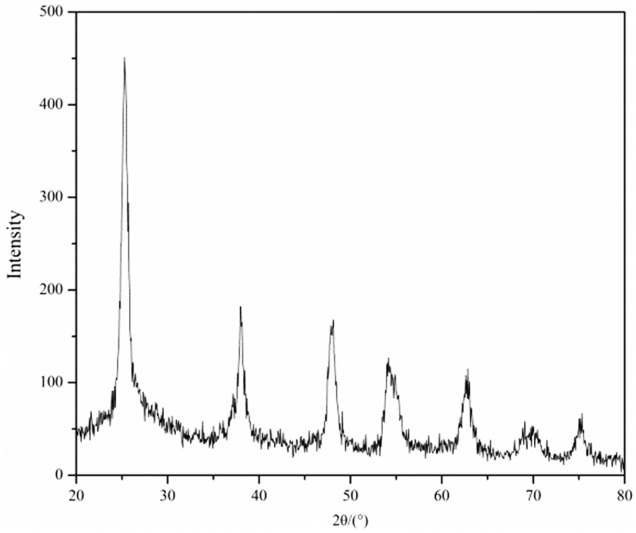

Fig. 1. XRD pattern of TiO_2 catalyst particles.

$$D = \frac{K\lambda}{\beta\cos\theta} \quad (2)$$

where D is the average crystal size (nm), K is the Scherrer constant (taken as 0.9), λ is the wavelength of X-ray (λ=1.5406 Å), β is the full peak width at half maximum for the most intense diffraction peak in the XRD pattern (at 2θ=25.3°), and θ is Bragg's diffraction angle. The calculated average size of anatase crystallite is 11.5 nm. The TiO_2 with smaller particle sizes and narrow particle size distribution was reported herein. Generally, smaller TiO_2 particles with high crystallinity are very beneficial to enhance the photocatalytic activity [24,32].

1-2. SEM

The surface morphology and topography of the prepared borosilicate glass supported TiO_2 photocatalysts was observed by scanning electron microscopy. As shown in Fig. 2, the prepared borosilicate glass supported TiO_2 exhibited a rough surface with almost homogenized particle size and shape. Plentiful TiO_2 particles were nearly uniformly dispersed on the surface of the borosilicate glass substrate and clearly visible. Similar results on immobilization of

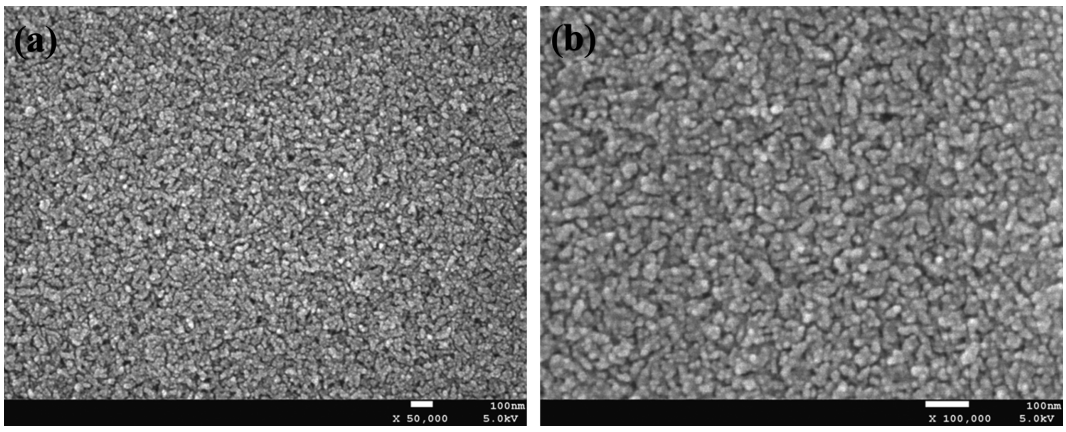

Fig. 2. SEM images of the borosilicate glass supported TiO_2.

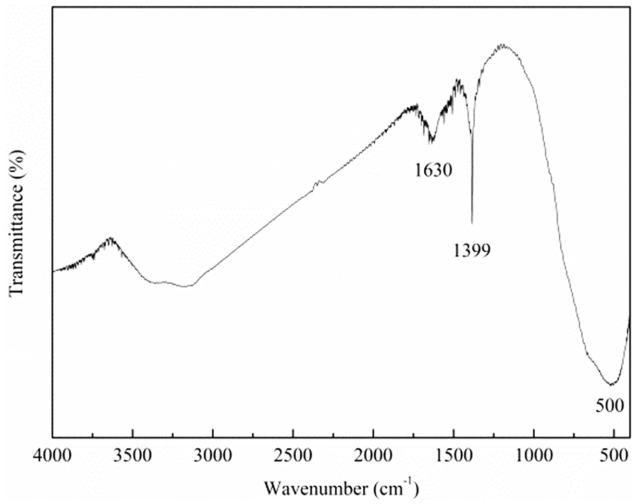

Fig. 3. FTIR spectra of TiO_2 catalyst particles.

TiO_2 have been reported on different supports [17,32,33]. According to the scale presented in the image, the size of TiO_2 particles was nanometer scale, which was approximately consistent with the XRD analyses. Such structural characteristic is beneficial in enhancing the photocatalytic activity.

1-3. FTIR

The functional groups of the prepared TiO_2 particles were measured by FTIR spectroscopic technique. The FTIR spectra of TiO_2 particles are shown in Fig. 3. The broad peaks at about 3,100-3,400 cm^{-1} corresponded to the stretching vibration of hydroxyl group and amine group. The strong absorption peaks observed at 1,630 cm^{-1} were related to bending vibration of hydroxyl groups from the unassociated H_2O on TiO_2 surface. Obviously, the hydroxyl groups and amine groups existed in the prepared TiO_2 due to the presence of water and NH_4^+. Surface hydroxylation is beneficial for the catalytic activity of TiO_2 due to enabling higher adsorption capacity for oxygen [6]. The characteristic peak at 500 cm^{-1} should be ascribed to stretching vibration of Ti-O bands in the TiO_2 lattice, demonstrating successful synthesis of the TiO_2. This result was consistent with the XRD analyses.

1-4. XPS

XPS was used to further study the chemical states of Ti and O in TiO_2 particles. The full survey spectrum and the high-resolution XPS spectra for TiO_2 particles are displayed in Fig. 4. As shown in Fig. 4(a), Ti, O, C and N are observed for TiO_2 particles in the full survey XPS spectrum. The full survey XPS spectrum mainly exhibits the peaks of Ti and O. The peak of C1s observed at 284.6 eV is related to C-C or adventitious carbon from the XPS instrument itself [34]. The peak of N1s located at 400 eV is due to the residual of NH_4^+ during washing process. Fig. 4(b) presents the high-resolution XPS spectrum of O1s in TiO_2 particles. The spectra displayed two peaks at 530.0 eV and 532.1 eV, respectively. The peak observed at 532.1 eV is attributed to the -OH groups on the surface of TiO_2, the peak centered at 530 eV is caused by the Ti-O bond in TiO_2 [35]. Fig. 4(c) presents high-resolution Ti 2p XPS spectra in TiO_2 particles. Two peaks at 458.5 eV and 464.1 eV can be ascribed to the Ti $2p_{3/2}$ and Ti $2p_{1/2}$ of TiO_2, respectively, indicating that Ti existed in the form Ti^{4+} [25,36,37]. The binding energy of Ti $2p_{3/2}$ for prepared TiO_2 was 0.3 eV larger than that of pure TiO_2 of 458.2 eV.

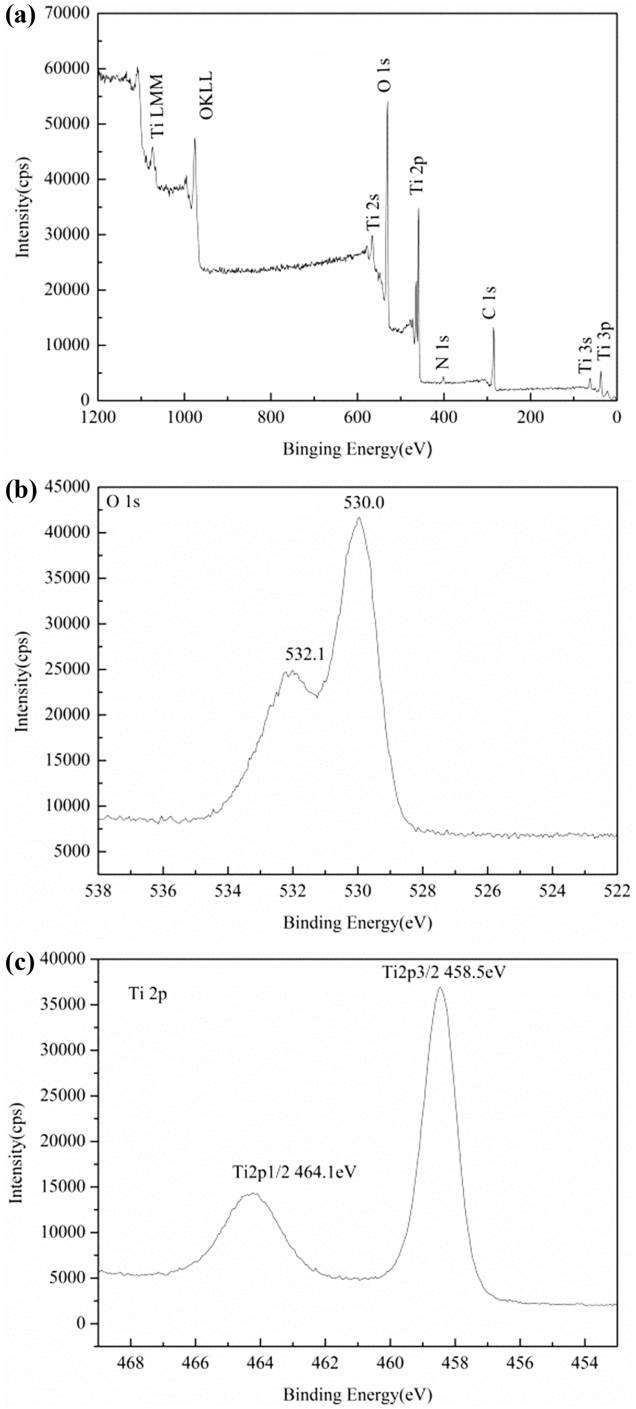

Fig. 4. The XPS spectra of TiO_2 catalyst particles.

2. Photocatalytic Degradation of CDNR

A CDNR degradation experiment was carried out in the dark space. It was found that the CDNR content of adsorption in dark space was small. The degradation efficiency of CDNR was about 3%. The photocatalytic degradation feasibility of CDNR by borosilicate glass supported TiO_2 was evaluated experimentally. The

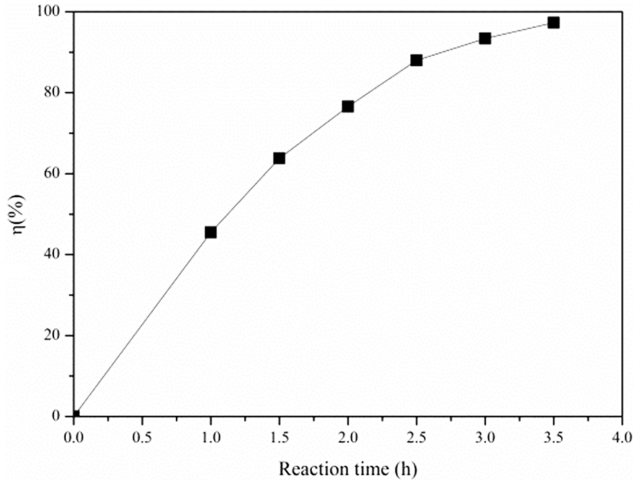

Fig. 5. Effect of reaction time on CDNR degradation.

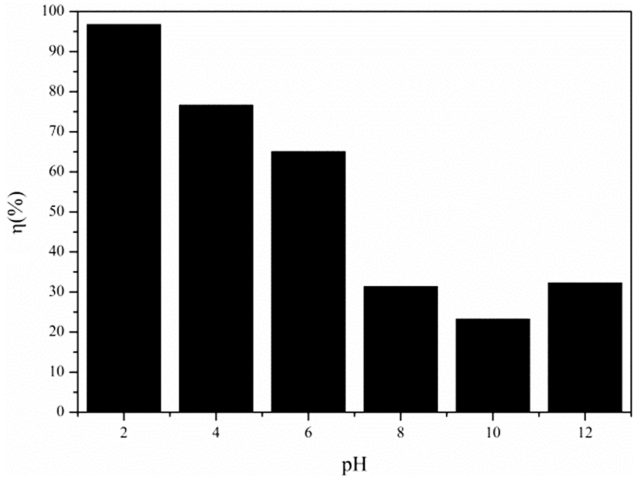

Fig. 6. Effect of pH on CDNR degradation.

degradation efficiency of CDNR from wastewater by photocatalytic oxidation was closely related to reaction conditions. Therefore, effects of reaction variables such as reaction time, pH value, TiO_2 dosage, CDNR concentration and Cl^- on the degradation efficiency of CDNR were investigated thoroughly in this paper.

2-1. Effect of Reaction Time

The reaction time plays an important role in the degradation efficiency. The effect of reaction time on degradation efficiency of CDNR at an initial CDNR concentration of 10 mg/L and NaCl concentration of 5.85% (w/w) was studied using 1 g/L of TiO_2 at a time interval of 0-3.5 h and pH 2 under UV irradiation. As depicted in Fig. 5, with an increasing reaction time, the degradation efficiency of CDNR showed a sharp increase and then changed slightly, which resulted from the depletion of CDNR in wastewater. The degradation efficiency of CDNR reached 97.7% after 3.5 h, demonstrating the good photocatalytic activity of the borosilicate glass supported TiO_2 for CDNR degradation from a salty wastewater. It was related to uniform anatase TiO_2 nanostructure. The CDNR concentration of wastewater after 3.5 h under ultraviolet irradiation met the national discharge standard, illustrating the feasibility of photocatalytic degradation for CDNR by borosilicate glass supported TiO_2. Therefore, 3.5 h was selected the reaction time for subsequent experiments.

2-2. Effect of pH

pH should be taken into account during degradation of CDNR, since it would adjust the charge properties on the surface of TiO_2 and CDNR, as well as the adsorption of CDNR on the surface of TiO_2. To investigate the effect of pH on the degradation efficiency of CDNR from wastewater by the borosilicate glass supported TiO_2 under UV light irradiation, degradation experiments were performed using 1 g/L of TiO_2 at different pH range from 2 to 12, an initial CDNR concentration of 10 mg/L and NaCl concentration of 5.85% (w/w) for 3.5 h under UV irradiation. The results are shown in Fig. 6. As can clearly be seen, the degradation of CDNR depended significantly on pH values. The degradation efficiency of CDNR decreased with the increase of pH value from 2 to 10, beyond which the degradation efficiency started to increase. Acidic pH values promoted photocatalytic degradation process in comparison to alkaline pH values. The pH influences the surface charge of TiO_2. The surface of TiO_2 is negatively charged at pH higher than the point of zero charge of TiO_2 (pH=6.5). In contrast, the surface of TiO_2 is positively charged at pH lower than the point of zero charge of TiO_2 [32,38]. CDNR molecules are anionic, surface positive charged TiO_2 at pH lower than 6.5 would enhance the electrostatic attraction effects between TiO_2 and CDNR molecules, and facilitate the contacting of the photon generated ·OH which governs the degradation process [39]. Thus, the degradation efficiency of CDNR decreased with the increase of pH value from 2 to 10. Although a reduced degradation efficiency of CDNR may be caused by repulsion between the CDNR and negatively charged TiO_2 at pH higher than 6.5, surface coverage by OH^- is increased to a certain extent. OH^- reacts with the holes and subsequently forms ·OH. A counterbalance between these two above-mentioned effects leads to a slight increase of degradation efficiency for CDNR. Thus, the degradation efficiency of CDNR increases with the increase of pH from 10 to 12. The highest degradation efficiency for CDNR was observed at pH 2. At pH 2, 97.7% of CDNR in wastewater was degraded after 3.5 h. Hence, other experiments were carried

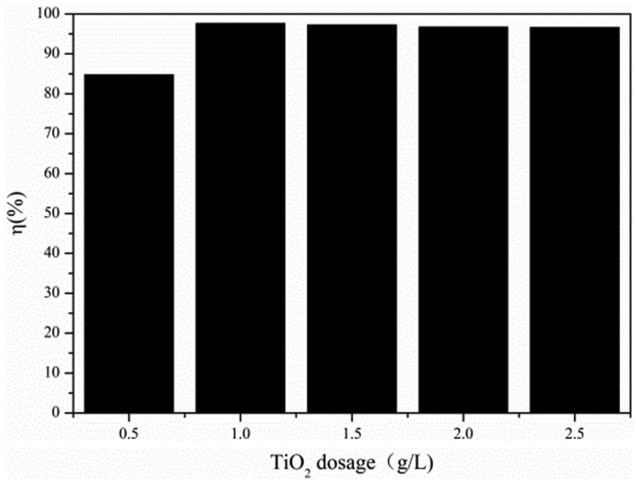

Fig. 7. Effect of TiO_2 dosage on CDNR degradation.

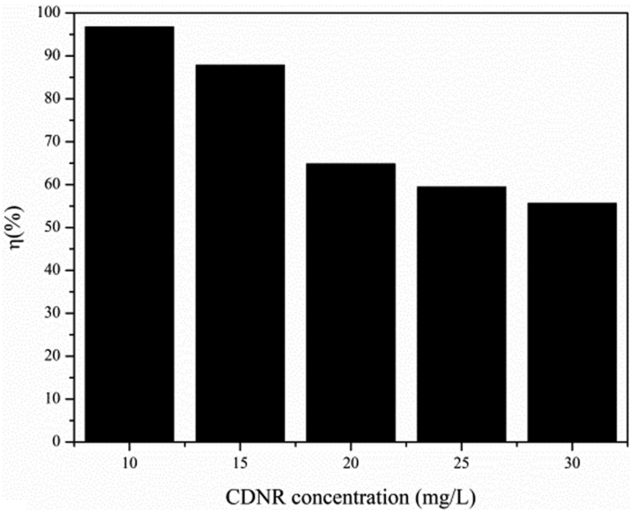

Fig. 8. Effect of CDNR concentration on CDNR degradation.

out at this pH.

2-3. Effect of TiO_2 Dosage

The optimization of photocatalyst dosage is essential to ensure high degradation efficiency and prevent the excess usage of catalysts, thus making the process more economical. The effect of TiO_2 dosage on the degradation efficiency of CDNR using TiO_2 dosage from 0.5 to 2.5 g/L at pH 2, an initial CDNR concentration of 10 mg/L and NaCl concentration of 5.85% (w/w) for 3.5 h under UV irradiation were illustrated in Fig. 8. It can be clearly observed that as TiO_2 dosage increased from 0.5 to 1 g/L, the degradation efficiency increased rapidly. Available free adsorption and catalytic sites are important for photocatalytic reactions. The increase of TiO_2 dosage increased the number of available adsorption and catalytic sites on the surface of TiO_2, resulting in more photon absorbed and CDNR adsorbed. Therefore, the degradation efficiency of CDNR is improved. The degradation efficiency of CDNR reached at least 95% when TiO_2 dosage was more than 1 g/L. However, the degradation efficiency decreased marginally when TiO_2 dosage was more than 1 g/L, which suggested that 1 g/L was an optimal TiO_2 dosage. This may be because excessive TiO_2 can trigger agglomeration on the surface of glass due to the inter-particle interaction effects, which would decrease the surface area and available free sites. In addition, excessive TiO_2 dosage decreased radiation efficiency by reducing the transmittance and inhibiting the photon absorption [32]. Consequently, the electron/hole pairs and the subsequent hydroxyl radicals are formed at a lower rate. In view of cost and degradation efficiency, the TiO_2 dosage of 1 g/L was selected for further experiments.

2-4. Effect of CDNR Concentration

With respect to practical application, the dependence of degradation efficiency of CDNR on the initial CDNR concentration is particularly important. The effect of initial CDNR concentration on degradation efficiency was investigated by varying the initial CDNR concentrations from 10 to 30 mg/L at pH 2, 1 g/L of TiO_2 and NaCl concentration of 5.85% (w/w) for 3.5 h under UV irradiation. The results are shown in Fig. 8. Clearly, the CDNR degradation efficiency decreased with the increase of initial CDNR concentration at higher level. As the CDNR concentration increased from 10 to 30 mg/L, the CDNR degradation efficiency decreased from 97.7 to 55.7%. Similar results have been reported for the photocatalytic degradation of 2-sec-butyl-4,6-dinitrophenol using TiO_2/SiO_2 aerogel composite photocatalysts [24] and aflatoxin B_1 [32]. This was probably due to available free sites of TiO_2 supplied to CDNR with higher concentration were deficient when TiO_2 dosage and light intensity were constant, which led to the decrease of CDNR adsorption fraction on the surface of TiO_2 and the probability of CDNR molecules to react with HO·. Additionally, the increase of the initial CDNR concentration would cause competitive adsorption of CDNR on the surface of TiO_2 and competitive absorption of photon by CDNR and TiO_2, thus preventing photons from reaching the surfaces of TiO_2 and reducing the generation of HO·. However, the trend of the CDNR amount removed normalized to the catalyst used was increased with the increase of initial CDNR concentration. Therefore, the initial concentrations of CDNR should be fully considered when optimizing the TiO_2 dosage for the best degradation efficiency.

2-5. Effect of Cl^-

Cl^- was a common constituent present in wastewater containing CDNR. Effect of Cl^- on degradation efficiency of CDNR by varying NaCl concentration from 0 to 5.85% (w/w) using borosilicate glass supported TiO_2 dosage 1.0 g/L at pH 2 and an initial CDNR concentration of 10 mg/L for 3.5 h under UV irradiation was particularly studied in this study. Fig. 9 shows the effect of Cl^- on degradation efficiency of CDNR. The degradation efficiency of CDNR was significantly enhanced by the presence of 5.85% NaCl in wastewater. The addition of NaCl to the mixture of aqueous CDNR up to 5.85% drastically increased the CDNR degradation efficiency from 86.6 to 97.7% in 3.5 h. The enhancement effect of Cl^- on CDNR degradation was in accordance with the previous report on the degradation of polycyclic aromatic hydrocarbons from offshore produced water by TiO_2 nanocatalyst [40]. This may be interpreted that wastewater samples with high salinity had higher ion strength and caused the salting-out effect, thus reducing the solubility of CDNR [40].

Previous studies reported the generation of $Cl^·$ and $Cl_2^{-·}$ in the

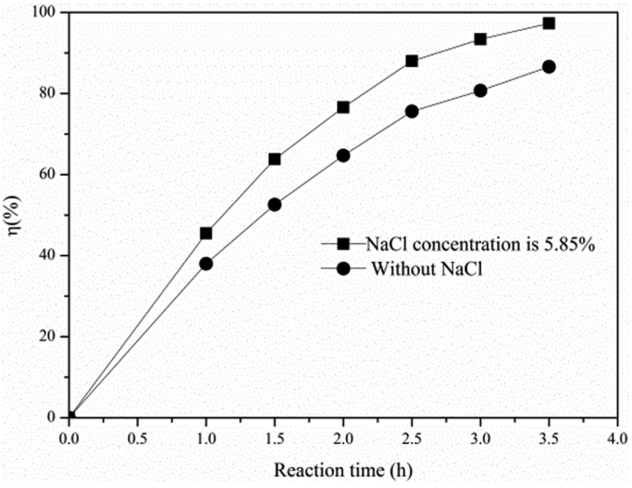

Fig. 9. Effect of Cl^- on CDNR degradation.

presence of Cl^- [41-44] as listed in Eqs. (3) to (6).

$$h^+ + Cl^- \rightarrow Cl^{\cdot} \quad (3)$$

$$HO^{\cdot} + Cl^- \rightleftharpoons ClOH^{\cdot-} \quad k_{for}=4.3\times10^9\ M^{-1}s^{-1};\ k_{rev}=6.1\times10^9\ M^{-1}s^{-1} \quad (4)$$

$$ClOH^{\cdot-} + H^+ \rightleftharpoons Cl^{\cdot} + H_2O \quad k_{for}=2.1\times10^{10}\ M^{-1}s^{-1};\ k_{rev}=2.5\times10^5\ M^{-1}s^{-1} \quad (5)$$

$$Cl^{\cdot} + Cl^- \rightleftharpoons Cl_2^{\cdot-} \quad k_{for}=6.5\times10^9\ M^{-1}s^{-1};\ k_{rev}=1.1\times10^5\ M^{-1}s^{-1} \quad (6)$$

where, k_{for} and k_{rev} represent the reaction rates of forward and backward reactions, respectively. Note that Cl^- might scavenge h^+/HO· and form weaker $Cl^{\cdot}/Cl_2^{\cdot-}$ only in acidic solution [45-47]. Since the pH values of the wastewater were both 2.0 with and without NaCl, Cl^- adsorbed directly at a hole (h^+) on the surface of TiO_2 due to electrostatic attraction effect and then reacted with h^+ to form $Cl^{\cdot}$ according to Eq. (3), thereby hindering the recombination of the electron-hole pairs and thus resulting in a higher yield of radicals. On the other hand, the k_{for} was less than the k_{rev} in Eq. (4), indicating that unless the consumption rate of $ClOH^{\cdot-}$ was larger than the k_{rev} in Eq. (4), HO· would be significantly regenerated. Surprisingly, acidic condition facilitated $Cl^{\cdot}$ formation by consuming $ClOH^{\cdot-}$ [44]. The k_{for} was larger than the k_{rev} in Eq. (5). Furthermore, the k_{for} in Eq. (5) was larger than the k_{rev} in Eq. (4). Therefore, the generation of $Cl^{\cdot}$ by reaction of Cl^- with HO· would be significant. $Cl^{\cdot}$ was a selective oxidant and its reactivity with acetic acid, benzoic acid and phenol can be higher than that of HO·. In addition, according to Eq. (6), Cl^- could react with $Cl^{\cdot}$ to form $Cl_2^{\cdot-}$, which was more selective and less reactive than HO· or $Cl^{\cdot}$ [48]. Meanwhile, the presence of chloride significantly enhanced the degradation rate of 4-tert-butylphenol by Fe(III)-EDDS/$S_2O_8^{2-}$/UV due to the increased concentration of HO· and the new formed radical $Cl_2^{\cdot-}$ which also had high reactivity with 4-tert-butylphenol [49]. Therefore, it seems likely that reduced CDNR solubility or hindered the electron-hole pairs recombination or increased $Cl^{\cdot}$ and $Cl_2^{\cdot-}$ concentrations with the presence of Cl^- and high reactivity of $Cl^{\cdot}$ and $Cl_2^{\cdot-}$ with CDNR can count for the promote effect of Cl^- on the degradation of CDNR by borosilicate glass supported TiO_2 under UV light irradiation.

3. Kinetic Study of Photocatalytic Degradation of CDNR

Generally, heterogeneous catalytic reaction is described by the Langmuir-Hinshelwood kinetic model [16]. Typically, the photocatalytic reaction belongs to heterogeneous catalytic reaction. Therefore, the photocatalytic process can be described by the Langmuir-Hinshelwood kinetic model as the following equation:

$$r = -\frac{dC}{dt} = \frac{k_r K_{ad} C}{1 + K_{ad} C} \quad (7)$$

where r is the reaction rate (mg/L min), k_r is the rate constant of photocatalysis (mg/L min), K_{ad} is the adsorption equilibrium constant (L/mg), and t is the time in hour.

Integrating Eq. (7), the linearized expression Langmuir-Hinshelwood model can be given as follows:

$$\ln\frac{C_0}{C} + k_r(C_0 - C) = k_r K_{ad} t \quad (8)$$

When the concentration of reactant is low or the adsorption is relatively weak in the process of photocatalytic degradation, Eq. (8) can be simplified to a pseudo-first order reaction kinetic in the following form:

$$\ln\frac{C_0}{C} = k_r K_{ad} t = kt \quad (9)$$

where k is the apparent reaction rate constant.

In this study, the photocatalytic degradation kinetics of CDNR was investigated. Pseudo-first order kinetic was plotted according to Eq. (9). Fig. 10 shows plots of $\ln(C_0/C)$ versus time using initial CDNR concentration of 10 mg/L and varying photocatalyst dosage. All the plots were linear with R^2 (correlation coefficient) values, average 0.9488, suggesting that the photocatalytic degradation of CDNR under UV irradiation followed the pseudo-first order reaction kinetics. The slight deviation from linearity can originate from the agglomeration of TiO_2 and the presence of one of the reactants not in sufficiency large excess [50]. The values of k at different TiO_2 dosage were calculated according to the slopes of the

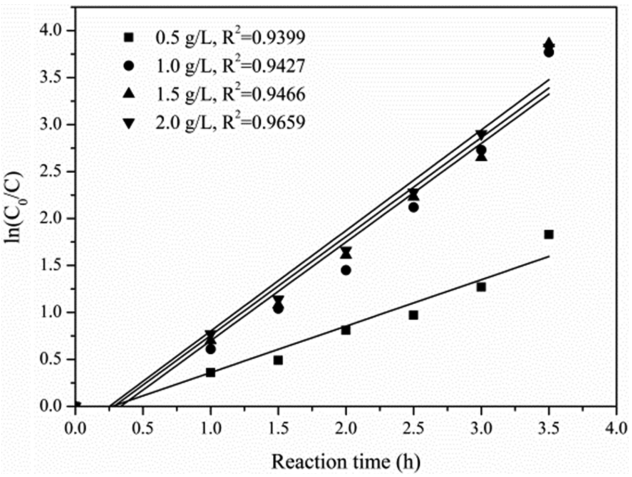

Fig. 10. Plot of pseudo-first order kinetics of CDNR photocatalytic degradation at different TiO_2 dosage.

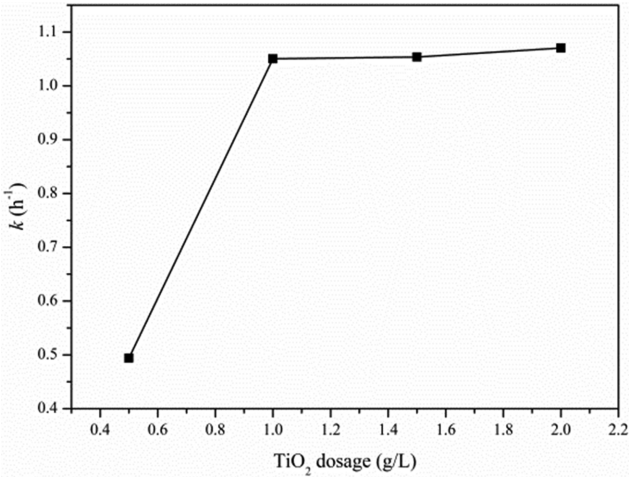

Fig. 11. The reaction rate constants at different TiO_2 dosage.

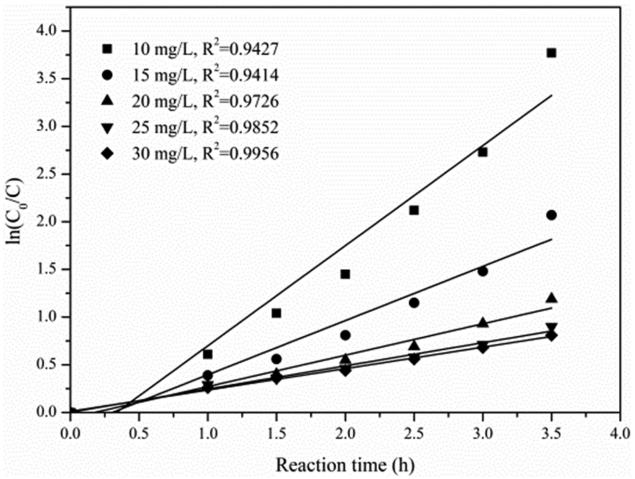

Fig. 12. Plot of pseudo-first order kinetics of CDNR photocatalytic degradation at different initial CDNR concentrations.

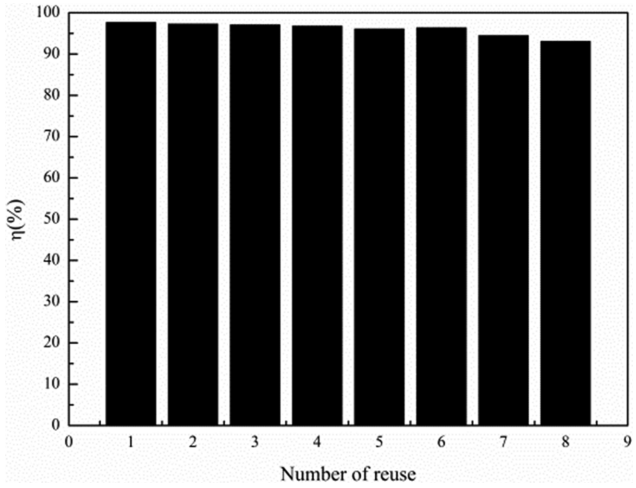

Fig. 14. Eight-cycle tests for degradation of CDNR.

fitted lines and plotted in Fig. 11. As the TiO_2 dosage increased from 0.5 to 1.0 g/L, k increased from 0.49 to 1.05 h^{-1}. This can be due to increase in the number of available adsorption and catalytic sites, as discussed in section 3.2.3. However, k increased at a relatively slow rate when TiO_2 dosage increased (above 1.0 g/L). This difference can be attributed to the fact that excessive TiO_2 can trigger agglomeration on the surface of glass, thereby generating a slight increase in the photoactivity area.

Fig. 12 provides plots of $\ln(C_0/C)$ versus time using optimum photocatalyst dosage of 1.0 g/L at different initial CDNR concentrations. All plots were linear with correlation coefficient (R^2) being average 0.9675. Therefore, the photocatalytic degradation of CDNR at different initial concentrations followed pseudo-first order kinetics. The calculated apparent reaction rate constant values are plotted in Fig. 13. As can be seen, by an increase in initial CDNR concentration, k decreased over the studied concentration range. This can be due to blocking of the photocatalytically active sites on the surface of TiO_2, thereby reducing the interaction of photons with these sites. Additionally, a fraction of light may be absorbed by the CDNR molecules rather than TiO_2 photocatalyst for high CDNR concentration, which can also reduce k to a certain extent.

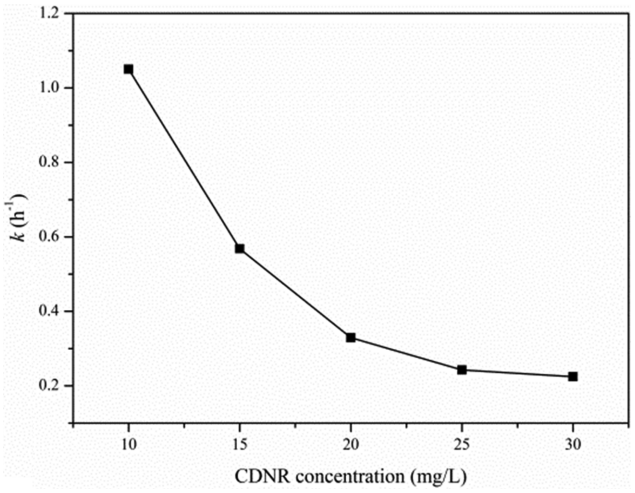

Fig. 13. The reaction rate constants at different initial CDNR concentrations.

4. Reusability Test

The reusability is a crucial property for practical application of a structured photocatalyst because it allows for multiple uses and thus reduces cost. To evaluate the reusability performance of the prepared borosilicate glass supported TiO_2, the cycling experiments were also carried out at the optimum conditions. For each new cycle, the borosilicate glass supported TiO_2 was collected from the aqueous solution, washed with water and utilized for the next cycle while keeping other reaction conditions unchanged. The degradation efficiency of CDNR with different cycles is shown in Fig. 14. As can be seen, the photocatalytic activity of borosilicate glass supported TiO_2 decreased slightly among the cycles. This may be attributed to the formation of by-products and their accumulation in the cavities and on the active surface sites of TiO_2. Noticeably, the degradation efficiency of CDNR using borosilicate glass supported TiO_2 maintained still higher than 90% after eight cycles, which made the application of borosilicate glass supported TiO_2 for CDNR wastewater treatment more practical. This indicates that the photocatalytic activity of the borosilicate glass supported TiO_2 has good reusability.

CONCLUSION

The feasibility of photocatalytic degradation of CDNR from industrial wastewater by borosilicate glass supported TiO_2 was evaluated. Borosilicate glass supported TiO_2 was prepared by a novel sol-gel route via dip-coating method. The XRD results indicated that TiO_2 prepared at low temperature was anatase TiO_2 and effective for photocatalytic degradation of CDNR in wastewater. SEM images showed that the borosilicate glass supported TiO_2 was uniform without surface aggregates. The effects of reaction time, pH value, TiO_2 dosage, CDNR concentration and Cl^- on CDNR degradation were investigated. The degradation efficiency increased with increasing irradiation time. Furthermore, the CDNR degradation efficiency decreased with the increase of CDNR concentra-

tion from 10 to 30 mg/L, decreased with the pH value increase to 10 at first and then increased with pH value over 10. The degradation efficiency increased with TiO_2 dosage. However, excess TiO_2 inhibited the degradation of CDNR. Chloride ions can promote the photocatalytic reaction in this study. The reusability of borosilicate glass supported TiO_2 was also evaluated and a promising photocatalytic performance was observed with a very slow variation of the decay rate after eight consecutive usages. At pH 2, reaction time 3.5 h, CDNR concentration 10 mg/L and TiO_2 dosage 1.0 g/L, 97.7% of CDNR was degraded in the presence of Cl^- with an apparent reaction rate constant of 1.05 h^{-1}. Hence, the CDNR in wastewater could be successfully degraded by borosilicate glass supported TiO_2. This study offers a low-cost eco-friendly solution to degrading CDNR in industrial wastewater.

ACKNOWLEDGEMENTS

This work was financially supported by Foundation of State Key Laboratory of High-efficiency Utilization of Coal and Green Chemical Engineering (Grant No. 2017-K14), the Scientific and Technological Project of Henan Province (Grant No. 172102210007), the Postdoctoral Startup Research Fund of Zhengzhou University, the Postdoctoral Research Sponsorship in Henan Province (Grant No. 2015004), and the Startup Research Fund of Zhengzhou University (Grant No. 1411324018). The authors are also grateful to all anonymous reviewers who contributed to improving this work.

REFERENCES

1. R. Shi and Y. Huang, *J. Harbin Inst. Technol. New Ser.*, **15**, 518 (2008).
2. B. Wang, Y. Zhang, W. Jiang, J. Li and Q. Luo, *New Chem. Mat.*, **41**, 117 (2013).
3. X. Li, F. Qin, Q. Dai, S. Shao and X. Wang, *Res. Chem. Intermed.*, **44**, 6087 (2018).
4. J. Hu, Y. Huang and N. Jin, *Synth. Technol. Appl.*, **18**, 18 (2003).
5. G. Cai, D. Li, D. Fang and W. Yu, *Polym. Test.*, **40**, 143 (2014).
6. X. Wei, H. Wang, Z. Li, Z. Huang, H. Qi and W. Jiang, *Appl. Surf. Sci.*, **372**, 108 (2016).
7. M. Mich, US Patent, 5,001,279 (1991).
8. Y. Zhang, W. Jiang and Q. Yang, *China Ceram.*, **50**, 34 (2014).
9. H. Chaker, L. Cherif-Aouali, S. Khaoulani, A. Bengueddach and S. Fourmentin, *J. Photochem. Photobiol. A.*, **318**, 142 (2016).
10. K. Nakata and A. Fujishima, *J. Photochem. Photobiol. C.*, **13**, 169 (2012).
11. Y. Tang, S. Luo, Y. Teng, C. Liu, X. Xu, X. Zhang and L. Chen, *J. Hazard. Mater.*, **241-242**, 323 (2012).
12. X. Wang, Z. Wu, Y. Wang, W. Wang, X. Wang, Y. Bu and J. Zhao, *J. Hazard. Mater.*, **262**, 16 (2013).
13. S. I. Patsios, V. C. Sarasidis and A. J. Karabelas, *Sep. Purif. Technol.*, **104**, 333 (2013).
14. J. Sun, X. Yan, K. Lv, S. Sun, K. Deng and D. Du, *J. Mol. Catal. A-Chem.*, **367**, 31 (2013).
15. Z. Lu, F. Chen, M. He, M. Song, Z. Ma, W. Shi, Y. Yan, J. Lan, F. Li and P. Xiao, *Chem. Eng. J.*, **249**, 15 (2014).
16. Z. Lu, P. Huo, Y. Luo, X. Liu, D. Wu, X. Gao, C. Li and Y. Yan, *J. Mol. Catal. A- Chem.*, **378**, 91 (2013).
17. Z. Mohammadi, S. Sharifnia and Y. Shavisi, *Mater. Chem. Phys.*, **184**, 110 (2016).
18. A. Fernández, G. Lassaletta, V. M. Jiménez, A. Justo, A. R. González-Elipe, J.-M. Herrmann, H. Tahiri and Y. Ait-Ichou, *Appl. Catal. B-Environ.*, **7**, 49 (1995).
19. M. R. Espino-Estévez, C. Fernández-Podríguez, O. M. González-Díaz, J. A. Navío, D. Fernández-Hevia and J. M. Doña-Rodríguez, *Chem. Eng. J.*, **279**, 488 (2015).
20. B. Tryba, *J. Hazard. Mater.*, **151**, 62 (2008).
21. A. Shet and K. V. Shetty, *Environ. Sci. Pollut. Res.*, **23**, 20055 (2016).
22. J. Thomasa, S. Radhikaa and M. Yoonb, *J. Mol. Catal. A-Chem.*, **411**, 146 (2016).
23. A. Tolosana-Moranchel, D. Ovejero, B. Barco, A. Bahamonde, E. Díaz and M. Faraldos, *J. Environ. Chem. Eng.*, **7**, 103051 (2019).
24. H. Wang, W. Liang, W. Jiang, *Mater. Chem. Phys.*, **130**, 1372 (2011).
25. X. Wei, H. Wang, X. Wang and W. Jiang, *Appl. Surf. Sci.*, **426**, 1271 (2017).
26. H. Ichinose, M. Terasaki and H. Katsuki, *J. Sol-Gel Sci. Technol.*, **22**, 33 (2001).
27. R. Ludwichk, O. K. Helferich, C. P. Kist, A. C. Lopes, T. Cavasotto, D. C. Silva and M. Barreto-Rodrigues, *J. Hazard. Mater.*, **293**, 81 (2015).
28. L. Ge, M. Xu and H. Fang, *J. Sol-Gel Sci. Technol.*, **38**, 47 (2006).
29. J. Wu and C. Chen, *J. Photochem. Photobiol. A: Chem.*, **163**, 509 (2004).
30. H. Khan, A. K. Khalil, A. Khan, K. Saeed and N. Ali, *Korean J. Chem. Eng.*, **33**, 2802 (2016).
31. M. Tasbihi, I. Călin, A. Šuligoj, M. Fanetti and U. L. Štangar, *J. Photochem. Photobiol. A: Chem.*, **336**, 89 (2017).
32. S. Sun, R. Zhao, Y. Xie and Y. Liu, *Food Control*, **100**, 183 (2019).
33. J. R. Kim and E. Kan, *J. Eviron. Manage.*, **180**, 94 (2016).
34. S. Zhou, Y. Liu, J. Li, Y. Wang, G. Jiang, Z. Zhao, D. Wang, A. Duan, J. Liu and Y. Wei, *Appl. Catal. B-Environ.*, **158-159**, 20 (2014).
35. G. An, W. Ma, Z. Sun, Z. Liu, B. Han, S. Miao, Z. Miao and K. Ding, *Carbon*, **45**, 1795 (2007).
36. R. Hao, G. Wang, H. Tang, L. Sun, C. Xu and D. Han, *Appl. Catal. B-Environ.*, **187**, 47 (2016).
37. H.-P. Kuo, S.-W. Yao and W.-Y. Hsu, *Korean J. Chem. Eng.*, **34**, 73 (2017).
38. L. Elsellami, N. Hafidhi, F. Dappozze, A. Houas and C. Guillard, *Chinese J. Catal.*, **36**, 1818 (2015).
39. G. Xiao, H. Su and T. Tan, *J. Hazard. Mater.*, **283**, 888 (2015).
40. B. Liu, B. Chen, B. Y. Zhang, L. Jing, H. Zhang and K. Lee, *J. Environ. Eng.-Asce.*, **142**, 04016054 (2016).
41. M. Ziegmann, T. Doll and F. H. Frimmel, *Acta Hydroch. Hydrob.*, **34**, 146 (2006).
42. J. E. Grebel, J. J. Pignatello and W. A. Mitch, *Environ. Sci. Technol.*, **44**, 6822 (2010).
43. D. Kanakaraju, C. A. Motti, B. D. Glass and M. Oelgemöller, *Chemosphere*, **139**, 579 (2015).
44. X. Kong, J. Jiang, J. Ma, Y. Yang, W. Liu and Y. Liu, *Water Res.*, **90**, 15 (2016).
45. G. Li, T. An, J. Chen, G. Sheng, J. Fu, F. Chen, S. Zhang and H. Zhao, *J. Hazard. Mater.*, **138**, 392 (2006).
46. L. Huang, L. Li, W. Dong, Y. Liu and H. Hou, *Environ. Sci. Tech-*

nol., **42**, 8070 (2008).
47. W. Zhang, Y. Li, Y. Su, K. Mao and Q. Wang, *J. Hazard. Mater.*, **215-216**, 252 (2012).
48. J. Fang, Y. Fu and C. Shang, *Environ. Sci. Technol.*, **48**, 1859 (2014).
49. Y. Wu, A. Bianco, M. Brigante, W. Dong, P. Sainte-Claire, K. Hanna and G. Mailhot, *Environ. Sci. Technol.*, **49**, 14343 (2015).
50. A. Balcha, O. P. Yadav and T. Dey, *Environ. Sci. Pollut. Res.*, **23**, 25485 (2016).